Available online at www.sciencedirect.com
ScienceDirect
Carbohydrate Research 342 (2007) 65–70
Carbohydrate RESEARCH

Synthesis of methyl 4′-*O*-methyl-β-D-cellobioside-$^{13}C_{12}$ from D-glucose-$^{13}C_6$. Part 2: Solid-state NMR studies

Frank Malz,[a] Yuko Yoneda,[b] Toshinari Kawada,[c] Kurt Mereiter,[d] Paul Kosma,[b] Thomas Rosenau[b,*] and Christian Jäger[a,*]

[a]*Federal Institute for Materials Research and Testing, Division I.3, Working Group NMR Spectroscopy, Richard-Willstaetter-Str. 11, D-12489 Berlin, Germany*
[b]*University of Natural Resources and Applied Life Sciences Vienna (BOKU), Department of Chemistry, Muthgasse 18, A-1190, Vienna, Austria*
[c]*Kyoto Prefectural University, Graduate School of Agriculture, Sakyo-Ku, Shimogamo, Kyoto 606-8522, Japan*
[d]*Department of Chemistry, Vienna University of Technology, Getreidemarkt 9, A-1060 Vienna, Austria*

Received 8 June 2006; received in revised form 25 October 2006; accepted 6 November 2006
Available online 11 November 2006

Abstract—Double Quantum (DQ) NMR, which utilizes the magnetic dipole interaction between the ^{13}C atoms, was used for the complete assignment of the ^{13}C NMR resonances to the corresponding carbon ring positions for the monoclinic and triclinic allomorphs of methyl 4′-*O*-methyl-β-D-cellobioside-$^{13}C_{12}$(**1-$^{13}C_{12}$**), a cellodextrin model compound of cellulose ^{13}C-perlabeled at the cellobiose core. The through-space interactions were used to identify the direct chemical bonds between adjacent carbon atoms in the rings. More importantly, the ^{13}C NMR signals of the carbon sites C1′ and C4 involved in the glycosidic bond were identified. This allowed for the complete ^{13}C chemical shift assignment, that when combined with the X-ray crystallography data provides a complete characterization.

Keywords: Cellodextrins; Cellulose; Model compounds; Solid-state NMR; Glycosidic bond; ^{13}C Isotopic labeling

1. Introduction

The allomorphism of cellulose, the exact structure of the respective hydrogen bond networks and the changes of these networks upon swelling and dissolution processes are current 'hot topics' in cellulose chemistry and major challenges in polysaccharide analytics today. One way to tackle these problems is to use cellulose model compounds, from which the analytical results may be transferred to the polymer. This approach allows both: deriving first results on the polymer by analogy and sharpening the analytical tools with the help of 'easy-to-study' model compounds.

The disaccharide methyl 4′-*O*-methyl-β-D-cellobioside (**1**) was the first oligosaccharide model compound for cellulose to be found to crystallize also in two allomorphs.[1,2] Solid-state NMR characterization verified a significant effect of the crystal packing on the ^{13}C chemical shifts; even though the conformation of the individual molecules was quite similar in both crystalline phases as shown by XRD, their solid-state NMR chemical shifts showed appreciable differences.[2] The complete assignment of the NMR resonances to specific carbon atoms in the glucopyranose units requires that (i) the two subsets of six NMR resonances, belonging to either glucopyranose moiety, must be distinguished from each other and that (ii) in a subsequent step the C1′ and C4 resonances involved in the glycosidic bonds must be identified. This is the aim of the present paper.

It should be noted that the first task has already been solved in the past by various groups using ^{13}C-enriched

* Corresponding authors. Tel.: +49 30 8104 1131; fax: +49 30 8104 5599 (C.J.); e-mail addresses: thomas.rosenau@boku.ac.at; christian.jaeger@bam.de

0008-6215/$ - see front matter © 2006 Elsevier Ltd. All rights reserved.
doi:10.1016/j.carres.2006.11.005

cellulose samples and two-dimensional (2D) Double Quantum (DQ) NMR experiments based on homonuclear *J*-couplings.[3–10] However, no information is obtained on the glycosidic bond this way.

Considering that the assignment of glucopyranose units in cellulose allomorphs[11] is still a challenge and a matter of debate, it seemed indispensable that such a basic problem was solved for a relatively simple cellulosic model compound before the complex polymer case is addressed. The synthesis of **1-$^{13}C_{12}$**, a compound fully ^{13}C-labeled in both glucopyranose units, has been described.[12] We now focus on the complete assignment of all ^{13}C resonances to their specific positions in the glucopyranose units, including the direct observation of the glycosidic bond, that is, the identification of the C-4 and C-1′ atoms of the adjacent glucopyranose moiety, in both crystallographic modifications—the stable monoclinic $P2_1$ allomorph and the metastable triclinic $P1$ allomorph—of this cellulosic model compound.

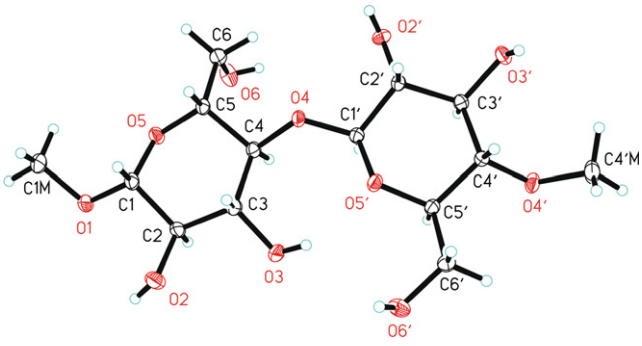

Figure 1. Thermal ellipsoid plots (60% ellipsoids) and crystallographic atom labeling of methyl 4′-*O*-methyl-β-D-cellobioside-$^{13}C_{12}$ (**1-$^{13}C_{12}$**).

2. Results and discussion

The molecular structure of compound **1-$^{13}C_{12}$** in its monoclinic phase[1,2] is shown in Figure 1 along with the crystallographic atom labeling, which is used in the following. Figure 2 displays the crystallographic packing along the *b*-axis.

The ^{13}C CPMAS NMR spectra of the monoclinic phase of the non-labeled model compound methyl 4′-*O*-methyl-β-D-cellobioside (**1**) and its labeled counterpart, methyl 4′-*O*-methyl-β-D-cellobioside-$^{13}C_{12}$ (**1-$^{13}C_{12}$**), are shown in Figure 3 (upper and middle row) together with the triclinic allomorph of **1-$^{13}C_{12}$** (lower row).[1,2] Narrow ^{13}C peaks with a line width at half-height of about 0.2 ppm (30 Hz) are observed for the non-labeled cellobioside (top-row spectrum) proving the high crystallinity of this sample. All of the 14 expected resonances are observed in this spectrum: 12 for the carbons in the two glucopyranose units and two for the methyl groups. These methyl resonances (C1M, C4′M) can be easily identified using different and, in particular, short CP times of about 0.5 ms. As the methyl groups rotate, the heteronuclear ^{1}H–^{13}C-dipole interaction within the methyl group is smaller than the corresponding coupling of the CH and CH_2 units. Consequently, the C1M and C4′M methyl carbon signal intensities are smaller for short CP times. These peaks are found at 55.7 ppm (right line) and at 61.4 ppm (third line from the right). All 12 carbon resonances of the glucopyranose rings are resolved. The pairs of the C1, C4, and C6 carbons can be assigned readily as shown in Figure 3 by comparing their chemical shifts with the well established assignment of celluloses.[8,13–15] However, without additional information it cannot be decided, which of these peaks represent the C1, C4, C6, or C1′, C4′, C6′ sites in the structure.

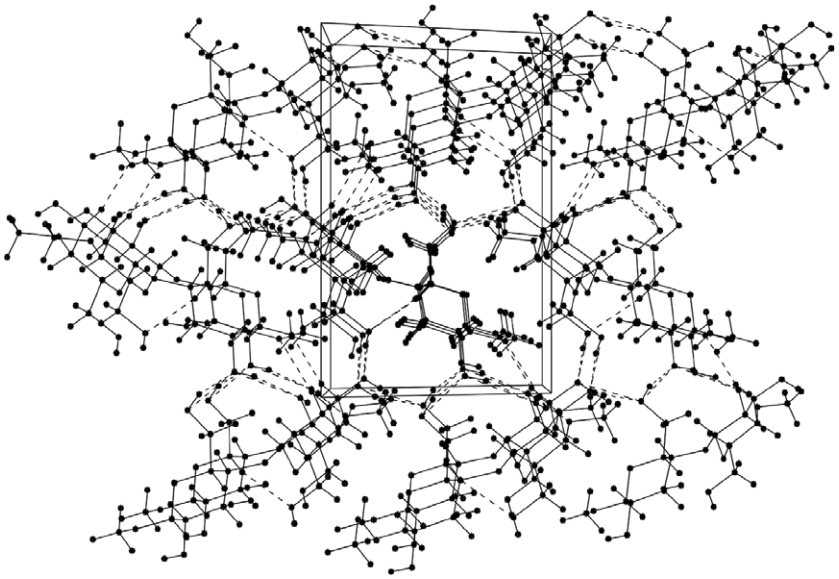

Figure 2. Crystal packing diagram of methyl 4′-*O*-methyl-β-D-cellobioside-$^{13}C_{12}$ (**1-$^{13}C_{12}$**), monoclinic allomorph, along the *b*-axis.

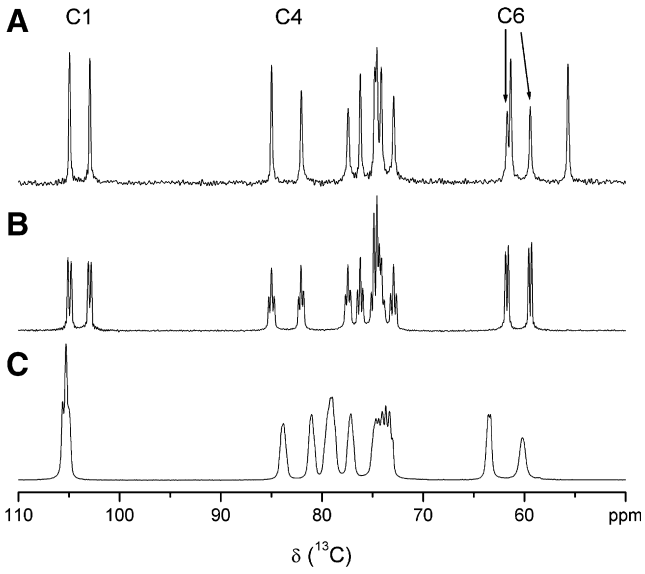

Figure 3. Proton-decoupled ^{13}C NMR CPMAS solid-state spectra of crystalline **1** (monoclinic phase) in natural ^{13}C abundance (A), and of **1-^{13}C$_{12}$** with >99% ^{13}C enrichment at the 12 cellobiose carbons (B: monoclinic phase, C: triclinic phase).

Furthermore, the assignment of the six ^{13}C resonances between 70 and 80 ppm to the C2, C2′, C3, C3′, C5, and C5′ sites is also not obvious.

The ^{13}C NMR spectrum of the monoclinic form of the ^{13}C enriched sample (**1-^{13}C$_{12}$**) is shown in the middle row of Figure 3. For comparison, the ^{13}C NMR spectrum of the enriched triclinic allomorph of **1-^{13}C$_{12}$** is shown at the bottom row of Figure 3. The most notable difference between the spectra of the two labeled cellobiose phases is that the peaks are somewhat broadened in the triclinic phase, which is attributed to a less perfect crystallinity of this sample. Further, the two C1/C1′ resonances have obviously very similar isotropic ^{13}C chemical shifts, in contrast to those in the monoclinic sample. Apart from evident minor chemical shift differences, all other features are similar for the two allomorphs.

Because of the isotopic enrichment (>99% ^{13}C) all observed ^{13}C resonances of the labeled samples appear as multiplets due to homonuclear *J*-couplings. Each of the C1, C1′, C6, and C6′ peaks consists of a doublet as there is only one directly bonded carbon. The typical *J*-coupling value is between 35 and 42 Hz. All other carbon resonances show a triplet-like shape suggesting that the two *J*-couplings to the two adjacent carbon atoms are of the same size. A fine structure owing to slightly different couplings was not observed in the solid-state NMR spectra. It should be mentioned that the C1M and C4′M sites were not ^{13}C-enriched in the synthesis. Consequently, their resonances do not show up in the spectrum of the labeled compound. Their absence confirms the above assignment of C1M/C4′M versus the C6/C6′ sites by different CP times.

Two-dimensional NMR experiments[16] are required to assign the ^{13}C NMR shifts to specific positions in the structure. Double Quantum (DQ) NMR experiments are particularly useful provided ^{13}C-enriched samples are available. Rather than exploiting the ^{13}C homonuclear *J*-couplings[16] where only directly bound carbon sites are detected—the homonuclear dipole coupling between the carbon atoms is used here. It should be noted, that the homonuclear *J* couplings, although not used for the DQ coherence generation, occur in the DQ peaks in both frequency dimensions, too. Hence, the DQ peaks will show multiplets on both frequency dimensions.

Under the experimental conditions of 12.5 kHz sample rotation frequency and a DQ evolution/reconversion time of one rotor period, the DQ peaks of *directly* bonded carbon atoms dominate the spectrum. Hence, the connectivity patterns of the rings carbons can be readily identified as shown in Figure 4.

A 2D DQ spectrum correlates the chemical shifts *a* and *b* of adjacent atoms, which are either chemically bonded or in close spatial proximity, along the horizontal axis (here the normal ^{13}C scale) with their sum (DQ) frequency $a + b$ on the vertical axis. A DQ peak pair will appear located at the crossing points of the DQ frequency $a + b$ along the vertical axis with the two peaks at frequencies *a* and *b* at the horizontal axis. The cross-peak pattern of sample **1-^{13}C$_{12}$** (monoclinic) is shown in

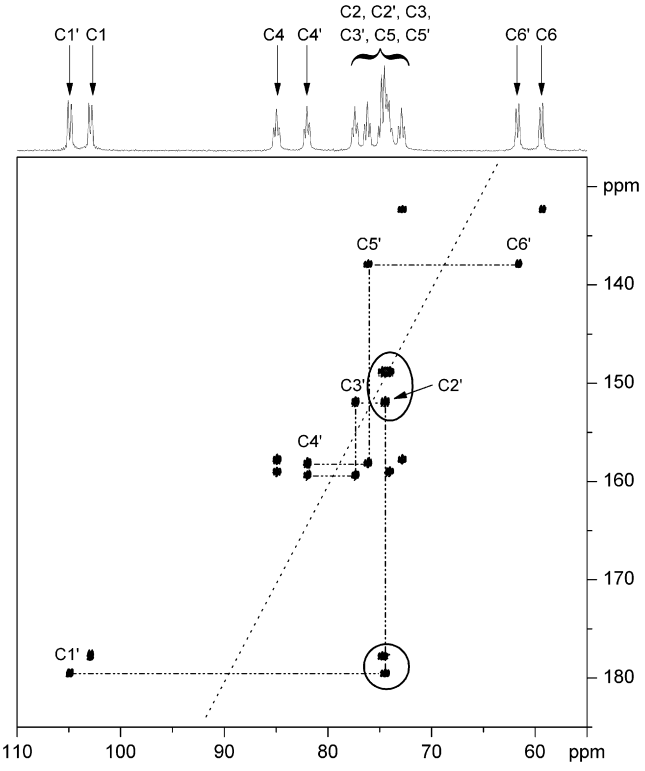

Figure 4. 2D ^{13}C Double Quantum (DQ) NMR spectrum of **1-^{13}C$_{12}$** (monoclinic) as contour plot (lowest contour level 6%). For more details see text.

Figure 4. Furthermore, the so-called DQ-diagonal (dotted line) is an essential feature in these spectra. It correlates the single quantum resonance frequency with its double quantum frequency; hence, its slope is 2. As a consequence, all DQ peak pairs involving chemically different carbons (with different chemical shifts) appear symmetrically around this DQ diagonal. Only if connected sites have the same chemical shift, their DQ peaks lay directly on the DQ diagonal. This is not the case with our samples.

In order to understand the assignment procedure for **1-$^{13}C_{12}$** (monoclinic), the ^{13}C CPMAS spectrum is shown on top of the 2D DQ spectrum. For clarity, the resolved and assigned carbon sites C1′, C1, C4, C4′, and C6′, C6 are displayed as well. The reason why the left peak of the anomeric carbons is assigned to C1′ and the left resonance of the C4/C4′ pair to C4 will be discussed later. This final assignment (consistent with the nomenclature of Fig. 1) requires the identification of the carbon signals involved in the glycosidic bond (see below). The lowest contour level used in Figure 4 is 6%. Under these circumstances, the spectrum of sample **1-$^{13}C_{12}$** (monoclinic) shows only DQ peaks for directly bonded carbons although the dipole coupling—acting through space—was used for the DQ generation and remixing. The procedure to find out, which of the carbon resonances belong to the same glucopyranose ring is relatively easy: Select for example the C6′–C5′ DQ peak pair located at the DQ frequency at 137.9 ppm. From the C5′ DQ peak go straight down until the C5′ peak of the C5′–C4′ DQ peak pair (symmetric around the DQ diagonal) is reached. This DQ peak pair is at a DQ frequency of 158.2 ppm. This simple procedure is repeated now for C4′/C3′ and so on until the C1′ site is identified. Figure 4 displays these DQ peak pairs for one of the glucopyranose rings (hatched lines). Sometimes the assignment requires some care if DQ frequencies of different pairs are very similar or if DQ peaks are very close to the DQ diagonal. The first case is met here for the C5′–C4′ and C5–C4 DQ peak pairs. Although the individual chemical shifts of C4/C4′ and C5/C5′ are quite different, their DQ frequencies differ only by 0.4 ppm (158.2 vs 157.8 ppm). But the fact that the DQ peaks pairs must be symmetric around the DQ diagonal readily solves the problem. Another case is marked by the ellipse at the center of the DQ spectrum. Here, the C3–C2 DQ peak pair is extremely close to the DQ diagonal, because the C3 and C2 chemical shifts are almost identical. Even if ^{13}C resonances of carbons in different rings (here C2 and C2′, ellipse at the bottom of Fig. 4) have nearly the same shifts, they can easily be separated through the DQ peaks with their C1 and C1′ neighbors. As a result, the ^{13}C resonances can be grouped into two classes corresponding to the two non-equivalent glucopyranose rings. The chemical shifts for the carbons of the two rings of **1-$^{13}C_{12}$** (monoclinic) are summarized in Table 1. It should be noted that similar results have been published for cellulose.[5,6,8,13]

Table 1. A complete assignment of the ^{13}C chemical shifts (δ) in the two glucopyranose rings of the monoclinic modification of **1-$^{13}C_{12}$**

	Chemical shifts δ (^{13}C) in ppm					
	C1	C2	C3	C4	C5	C6
Glucopyranose' ring	104.9	74.4	76.2	82.0	74.8	61.7
Glucopyranose ring	102.9	74.5	74.1	84.9	72.9	59.4

The numbering follows the nomenclature used in Figure 1 and correlates the ^{13}C NMR shifts with the crystallographic XRD data for the first time.

Finally, the question, which set of resonances belongs to which of the glucopyranose units of the crystallographic structure can be answered. This is synonymous with the question, which of the two 'C1' and two 'C4' resonances belongs to the carbons C1′ and C4 forming the glycosidic bond. Only this step enables the full correlation of the carbon resonances with the X-ray structure shown in Figure 1. As the DQ peaks were generated by the homonuclear dipole coupling DQ peak pairs between remote, that is not directly bonded carbons, within the rings can be observed. These remote DQ peaks, such as for instance C6′–C4′ or C1′–C3′ have only about 5% of intensity of the DQ peaks of directly bonded carbon atoms because of the larger distances and, hence, their much smaller mutual dipole coupling. These remote DQ peak can be visualized in the spectrum by changing the lowest contour level of the plot to 3%. Figure 5 shows the essential section of the DQ spectrum for identifying the NMR resonances of the two carbon sites C1′ and C4 of the glycosidic bond for sample **1-$^{13}C_{12}$** (monoclinic).

The ^{13}C NMR spectrum is plotted on top of the DQ pattern for referencing the carbon site assignment. Besides the very strong direct DQ peak pairs C1′/C2′ and C1/C2 (not connected in Fig. 5), four additional DQ peak pairs are found. These pairs are indicated by hatched lines. At the DQ frequency 175.8 ppm the DQ peak pair of C1 and C5 sitting in the same glucopyranose ring and spaced by the ring oxygen site is found. Similarly, it is possible to assign the C1′–C3′ DQ peak pairs at 179.5 ppm and the remote C1′–C5′ bonding scenario of the other glucopyranose ring. Most importantly, there is one single DQ peak pair at 189.8 ppm, which shows the C1′ and C4 resonances of the glycosidic bond. With this piece of information, the two sets of six carbon NMR resonances for each glucopyranose ring can be correlated directly for the first time with the X-ray structure as shown in Figure 1.

In the same way, the triclinic allomorph of **1-$^{13}C_{12}$** was investigated. These results are summarized in Table 2. It is interesting to note, that in the triclinic phase the C3 and C3′ shifts are almost identical (as is for C1 and C1′), and that they are significantly low-field shifted by about 5 ppm compared with the monoclinic phase.

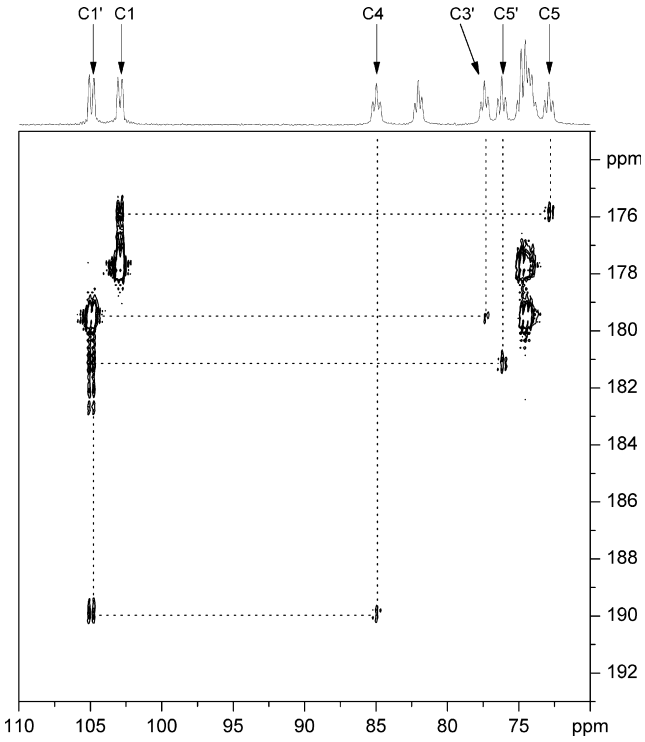

Figure 5. 2D ^{13}C Double Quantum (DQ) NMR spectrum of **1-$^{13}C_{12}$** (monoclinic) as contour plot (lowest contour level 3%). For more details see text.

Table 2. A complete assignment of the ^{13}C chemical shifts (δ) in the two glucopyranose rings for the triclinic modification of **1-$^{13}C_{12}$**

	Chemical shifts δ (^{13}C) in ppm					
	C1	C2	C3	C4	C5	C6
Glucopyranose' ring	105.1	74.0	79.3	81.0	77.1	63.4
Glucopyranose ring	105.5	73.3	78.8	83.8	74.7	60.0

The numbering follows the nomenclature used in Figure 1 and correlates the ^{13}C NMR shifts with the crystallographic XRD data for the first time.

3. Conclusions

All solid-state NMR carbon resonances of the cellulose model compound methyl 4′-*O*-methyl-β-D-cellobioside-$^{13}C_{12}$ (**1-$^{13}C_{12}$**) in both its monoclinic and triclinic crystal phases were fully assigned using Double Quantum (DQ) NMR. For the first time, the connectivity of the carbon atoms forming the glycosidic bond, C1′ and C4, was observed directly.

In future studies, these NMR techniques will be used to study the interaction of the labeled model compound with cellulose solvents such as *N*,*N*-dimethylacetamide/LiCl or *N*-methylmorpholine-*N*-oxide, especially with regard to swelling as the initial stage in the dissolution process. Emphasis will be placed on the identification of interaction sites between solvent and solute molecules.

4. Experimental

4.1. NMR spectroscopic study

^{1}H and ^{13}C solid-state NMR measurements were performed on an AVANCE 600 spectrometer (14.1 T, Bruker Biospin GmbH, Rheinstetten, Germany) equipped with wide bore magnet. Magic angle sample spinning (MAS) was applied using 2.5 mm zirconia rotors. All MAS experiments were carried out at room temperature.

The ^{1}H NMR spectra were acquired at a Larmor frequency of 600.2 MHz using a 90° pulse. A rotor-synchronized echo was used for the spectra acquisition with a MAS spinning frequency of 27 kHz. The spectra were acquired by one scan with 2k data points at a spectral width of 100 kHz. The relaxation delays were varied (1, 2, 10, 20, 30, 60, 90, 120, 240, 480, and 720 s) and a ^{1}H T_1 of about 120 s was measured.

^{13}C CPMAS spectra were recorded at a Larmor frequency of 150.9 MHz with a 2.5 mm double-resonance probe. Cross-polarization (CP)[17] was used for the spectra acquisition. The ^{1}H 90° pulse length was 2.75 μs, a contact time of 2 ms was used with repetition times of 30 s. During the contact time, the carbon spin lock field strength was held constant, while the proton spin-lock field was ramped linearly (ramped-CP[18]) down to 50% of the initial value. Proton decoupling was carried out with a 15° two pulse phase modulation (TPPM) sequence.[19] For ^{13}C chemical shifts (δ) the glycine COOH signal set to $\delta = 176.4$ ppm was used.

Two-dimensional homonuclear ^{13}C Double Quantum (DQ) experiments using the back-to-back sequence[20] were carried out at a MAS spinning frequency of 20 kHz. The ^{1}H 90° pulse length was 2.00 μs, a contact time of 1 ms was used for cross-polarization (CP). Proton decoupling was carried out with a two pulse phase modulation (TPPM) sequence. Rotor-synchronized t_1 incrementation ($\Delta t_1 = 50$ μs) was used. In total $1024t_1$ increments were acquired with 16 scans per increment and a repetition time of 10 s.

4.2. X-ray crystallographic study

X-ray data collection was performed with a Bruker AXS Smart APEX CCD diffractometer and graphite monochromatized Mo K_α radiation, $\lambda = 0.71073$ Å at 100 K; corrections for absorption and related effects with the program SADABS, structure solution with direct methods, structure refinement on F^2 (Bruker AXS, 2001: programs SMART, version 5.626; SAINT, version 6.36A; SADABS version 2.05; XPREP, version 6.12; SHELXTL, version 6.10. Bruker AXS Inc., Madison, WI, USA).

Methyl 4′-*O*-methyl-β-D-cellobioside-$^{13}C_{12}$ (**1-$^{13}C_{12}$**). $^{12}C_2{}^{13}C_{12}H_{26}O_{11}$, $M = 382.36$, monoclinic, space group $P2_1/c$ $a = 6.5846(5)$ Å, $b = 14.0141(12)$ Å, $c = 9.2868(8)$ Å, $\beta = 109.110(1)°$, $V = 809.73(12)$ Å^3,

$Z = 2$, $D_c = 1.519$ g/cm^3, $T = 100$ K, $\mu = 0.132$ mm^{-1}, $F(000) = 396$, colorless block ($0.46 \times 0.38 \times 0.24$ mm); total reflections = 12,058, unique reflections = 4686, R_{int}=0.0239, final refinement: data/restraints/parameters = 4686/79/250, goodness-of-fit on $F^2 = 1.038$, $R_1 = 0.0350$ ($I > 2\sigma(I)$), $wR_2 = 0.0875$ (all data).

CCDC 626358 contains the supplementary crystallographic data for this paper. These data can be obtained free of charge at www.ccdc.cam.ac.uk/conts/retrieving.html [or from the Cambridge Crystallographic Data Centre, 12, Union Road, Cambridge CB2 1EZ, UK; fax: (intl.) +44-1223/336-033; e-mail: deposit@ccdc.cam.ac.uk].

Acknowledgments

The financial support of the Fonds zur Förderung der wissenschaftlichen Forschung (FWF), (Project P17426-N11 to T.R.) is gratefully acknowledged.

References

1. Mackie, I. D.; Röhrling, J.; Gould, R. O.; Pauli, J.; Jäger, C.; Walkinshaw, M.; Potthast, A.; Rosenau, T.; Kosma, P. *Carbohydr. Res.* **2002**, *337*, 161–166; Corrigendum: *Carbohydr. Res.* **2002**, *337*, 1065.
2. Rencurosi, A.; Röhrling, E.; Pauli, J.; Potthast, A.; Jäger, C.; Perez, S.; Kosma, P.; Imberty, A. *Angew. Chem., Int. Ed.* **2002**, *41*, 4277–4281.
3. Brown, S. P.; Emsley, L. *J. Magn. Reson.* **2004**, *171*, 43–47.
4. Lesage, A.; Bardet, M.; Emsley, L. *J. Am. Chem. Soc.* **1999**, *121*, 10987–10993.
5. Kono, H.; Yunoki, S.; Shikano, T.; Fujiwara, M.; Erata, T.; Takai, M. *J. Am. Chem. Soc.* **2002**, *124*, 7506–7511.
6. Kono, H.; Erata, T.; Takai, M. *Macromolecules* **2003**, *36*, 5131–5138.
7. Kono, H.; Numata, Y.; Erata, T.; Takai, M. *Macromolecules* **2004**, *37*, 5310–5316.
8. Kono, H.; Numata, Y. *Polymer* **2004**, *45*, 4541–4547.
9. Cadars, S.; Lesage, A.; Emsley, L. *J. Am. Chem. Soc.* **2005**, *127*, 4466–4476.
10. De Paepe, G.; Giraud, N.; Lesage, A.; Hodgkinson, P.; Bockmann, A.; Emsley, L. *J. Am. Chem. Soc.* **2003**, *125*, 13938–13939.
11. Kono, H.; Numata, Y. *Cellulose* **2006**, *13*, 317–326.
12. Yoneda, Y.; Kawada, T.; Rosenau, T.; Kosma, P. *Carbohydr. Res.* **2005**, *340*, 2428–2435.
13. Numata, Y.; Kono, H.; Kawano, S.; Erata, T.; Takai, M. *J. Biosci. Bioeng.* **2003**, *96*, 461–466.
14. Tang, H. R.; Belton, P. S. *Solid State Nucl. Magn. Reson.* **2002**, *21*, 117–133.
15. Atalla, R. H.; VanderHart, D. L. *Solid State Nucl. Magn. Reson.* **1999**, *15*, 1–19.
16. Lesage, A.; Steuernagel, S.; Emsley, L. *J. Am. Chem. Soc.* **1998**, *120*, 7095–7100.
17. Hartmann, S. R.; Hahn, E. L. *Phys. Rev.* **1962**, *128*, 2042–2053.
18. Metz, G.; Wu, X. L.; Smith, S. O. *J. Magn. Reson., Ser. A* **1994**, *110*, 219–227.
19. Bennett, A. E.; Rienstra, C. M.; Auger, M.; Lakshmi, K. V.; Griffin, R. G. *J. Chem. Phys.* **1995**, *103*, 6951–6958.